Structure refinements of some thermally disordered dolomites

R. J. REEDER

Department of Earth and Space Sciences
State University of New York at Stony Brook
Stony Brook, New York 11794

AND H.-R. WENK

Department of Geology and Geophysics
University of California, Berkeley, California 94720

Abstract

Single crystal X-ray structure refinements of one ideally ordered and two partially disordered dolomites provide structural data about the thermally induced, cation disordering process. Most refined parameters show progressive and gradual changes as disorder increases. It was found that completely disordered crystals could not be recovered using piston-cylinder methods owing to reordering during the quench. This factor limited the range over which disorder in quenched specimens could be studied, although some parameters are extrapolated to complete disorder. New experiments confirm that disorder is complete by 1150°C.

Electron density maps based on intensity data from specimens which exceeded the critical disordering temperature suggest CO_3 group disorder of a rotational kind.

Introduction

Previous structural investigations of cation disordering in dolomite, $CaMg(CO_3)_2$, and other isostructural carbonates have been limited to X-ray powder methods. Consequently, information obtained from these studies was necessarily incomplete and actual cation site occupancies could not be determined. In the present study, we report the results of single-crystal X-ray structure refinements of one ideally ordered and two partially disordered dolomites. In addition, some observations are reported on intensity data obtained from two other dolomites which have undergone the $R\bar{3}c$ to $R\bar{3}$ transition during quenching.

Goldsmith and co-workers were the first to recognize the importance of cation disorder in dolomite and its effect on both low-temperature metastable behavior and high-temperature equilibrium behavior (Goldsmith and Graf, 1958; Goldsmith, 1959; Goldsmith and Heard, 1961). Goldsmith and Heard studied the cation disordering transformation over the temperature range 900° to 1250°C. They used an internally heated gas apparatus and squeezer-type techniques to anneal stoichiometric dolomite powders. High confining pressures (*i.e.*, high P_{CO_2}) were necessary to prevent decomposition to the oxides and vapor. They examined the quenched charges by powder camera X-ray diffraction methods to monitor the intensity of superstructure reflections ($h\bar{h}0l$, l = odd). They found a gradual and progressive weakening of these

reflections to above 1150°C. Goldsmith and Heard were unable to recover a completely disordered phase due to a rapid reordering reaction during the quench. However, they estimated a· critical disordering temperature at roughly 1200°C and concluded that the transformation was continuous or "higher-order" (a transition of the second kind in the Landau sense).

Subsequent to this, Goldsmith (1972) studied the cation disordering transformation in the isostructural $CdMg(CO_3)_2$, which behaves as a lower-temperature analog to dolomite. Using the methods described above, Goldsmith documented the gradual weakening of the superstructure reflections with increasing temperature and, finally, their disappearance at 825°C. For both $CaMg(CO_3)_2$ and $CdMg(CO_3)_2$, the disorder was assumed to be of a random, substitutional type and no evidence of mixed-layering type defects was found.

The present study was initiated in an attempt to quantify the disordering process for use in thermodynamic modeling. A knowledge of site occupancies as a function of temperature would also allow an evaluation of the Bragg–Williams model as used by Navrotsky and Loucks (1977). Persistent problems of back-reaction during quenching prevented obtaining the equilibrium distribution at temperature. However, the minimum degree of disorder at a given temperature is obtained, as well as a documentation of structural changes accompanying disordering.

Experimental methods

Starting material

The specimen used in this study was a large, optically clear, cleavage rhomb of dolomite from a metamorphic carbonate complex at Eugui, Spain. Crystal quality and symmetry were checked by Laue and precession photographs. A wet chemical analysis confirms that the composition is nearly stoichiometric (Table 1).

Examination of the Eugui dolomite by transmission electron microscopy (TEM) indicates that the material is homogeneous (Reeder and Nakajima, 1982) with very few dislocations (Barber *et al.*, 1981).

Thermal disordering

Cation disorder was produced by annealing specimens in a ¾" diameter, internally heated, piston-cylinder apparatus located at the University of Chicago. J. R. Goldsmith conducted the experiments in conjunction with a related project on the decomposition behavior of dolomite at high temperatures and pressures. Experimental methods are described in detail by Goldsmith (1980) and only salient aspects will be mentioned here.

In order to recover satisfactory single crystals, a mixture of small rhombs and powder of Eugui dolomite was packed in platinum capsules. These were crimped shut, but not sealed. The capsules were cushioned by powdered glass within "soft glass" assemblies. These precautions proved adequate, since satisfactory rhombs were routinely recovered from the run products.

The charges were slowly taken up in temperature and pressure and then allowed to equilibrate at final T and P for varying periods of time. Experimental conditions are given in Table 2. Four different annealing temperatures were chosen (1050°, 1100°, 1150° and 1200°C) on the basis of the temperature range over which the most significant disordering was found by Goldsmith and Heard. Samples were rapidly quenched by cutting power to the heating element. It is difficult to estimate the cooling rate, although it appears likely that a specimen cooled from 1200°C to 500°C in less than 10 seconds.

A portion of the powder from each run product was examined by X-ray powder diffraction to check for evidence of decomposition. None of the products from the

Table 2. Experimental conditions for annealing

Specimen	T (°C)	P (kbar)	Time at T (min.)
DO-1050	1050 ± 10	11	120
DO-1100	1100 ± 10	11	45
DO-1150	1150 ± 10	11	16
DO-1200	1200 ± 15	20	15

present study showed any trace of MgO. However, those samples equilibrated at 1150° and 1200°C (DO-1150 and DO-1200) revealed the presence of trace amounts of CaO (lime) suggesting either decomposition or partial melting (*cf.* Irving and Wyllie, 1975). Thus, the dolomites recovered from these two experiments may have deviated very slightly from ideal stoichiometry. In all powder patterns the superstructure reflections were either absent or very weak.

Optically-clear cleavage rhombs were separated from the products and suitable single crystal rhombs were mounted on glass needles for X-ray work. Precession and Laue photographs were obtained for purposes of checking orientation, symmetry, and quality of crystals. Superstructure reflections, although weak, were clearly visible on the precession photographs for all crystals. The run products were also examined by TEM to check for anomalous microstructures. Samples DO-1050 and DO-1100 both were homogeneous, but dislocations were far more common in these than in the starting material. DO-1150 and DO-1200 contained pervasive domains which have been interpreted as transformation-induced twin domains by Reeder and Nakajima (1982). During the quench, a symmetry change from $R\bar{3}c$ to $R\bar{3}$, corresponding to the appearance of long-range order, resulted in the formation of domains. Thus these two highest-temperature samples are thought to have lacked long-range order at their respective equilibration temperatures. Precession photographs of these crystals exhibit no new reflections, as the twin operation is a 180° rotation around a zone axis parallel to *a*. However, intensities of certain reflections are modified since they represent superposition of separate reflections from the two twin components. We do not report refined parameters for these twinned dolomites, but comment later on electron density maps and observed intensities.

Structure refinement

In addition to the two high-temperature run products, the structure of a crystal of the starting material was also refined for purposes of comparison and also for general interest. A crystal of the Eugui untreated sample (hereafter EU) was ground into a sphere for refinement; rhombs were used for the experimental products. Crystal dimensions are given in Table 3. An absorption correction

Table 1. Compositional data for Eugui dolomite

	Weight % oxide[1]	Mole ratio - MCO_3
CaO	30.65	1.001
MgO	21.70	0.987
MnO	0.08	0.002
FeO	0.41	0.010
	52.84	2.000

[1]Wet chemical analysis

Table 3. Crystal size and absorption corrections

Sample	Dimensions (mm)	Transmission factor		
		max.	min.	ave.
EU	0.24 (sphere)	0.741[1]	0.746	0.745
DO-1050	0.09 x 0.09 x 0.15	0.804[2]	0.901	0.863
DO-1100	0.06 x 0.07 x 0.10	0.885	0.932	0.914

[1]Spherical absorption correction
[2]Calculated from UC Berkeley Program ABSORB

Table 5. Refinement data for three dolomites

	EU	DO-1050	DO-1100
Total observations	992	864	1650
Independent observations	530	351	312
Unrejected observations	511	294	264
R factor	0.018	0.043	0.041
Weighted R factor	0.027	0.049	0.043
Weight factor A	0.03	0.03	0.05
Extinction coefficient*	0.241 E-5		

*Overall isotropic extinction coefficient (Zachariasen, 1967)

(Table 3) was applied to the intensity data although it did not change the results appreciably.

All crystals were mounted with an *a* axis coincident with the goniometer axis; thus *c* was perpendicular to the goniometer axis. Two different settings are possible for the dolomite cell, depending on the orientation of the CO_3 groups within a given layer (*cf.* Althoff, 1977); they are related by a 180° rotation around *a*. The choice of cells does not affect the results of the refinement, as long as the correct O positions are chosen.

Data were collected at room temperature on a Nonius CAD-3 computer-controlled, 4-circle diffractometer using graphite-monochromatized Mo$K\alpha$ radiation. Automatically-centered positions of at least 30 reflections were used to refine lattice parameters by least-squares methods (Table 4). An independent determination of lattice parameters for the starting material (Eugui dolomite) was made using a Jagodzinski–Guinier camera. The *c* cell parameter determined by this method ($c = 16.004(1)$Å) is within the error of the value determined from diffractometer data. However, the *a* cell parameter determined by the camera method ($a = 4.8073(5)$Å) is larger than is consistent with the error of the diffractometer value, $4.8038(9)$Å. We note this discrepancy but choose to retain the values determined from the diffractometer data for internal consistency.

Table 4. Lattice parameters and cell volumes of the untreated and annealed dolomites.

	a (Å)	*c* (Å)	V_{cell} (Å³)
EU	4.8038(9)*	16.006(4)	319.88 (8)
DO-1050	4.805 (2)	16.015(9)	320.22(22)
DO-1100	4.805 (2)	16.022(8)	320.36(21)
DO-1150	4.798 (2)	15.993(8)	318.85(19)
DO-1200	4.799 (2)	15.986(7)	318.84(18)

*Estimated standard deviations in parentheses.

Intensity data were collected using the θ–2θ scan technique with a scan width of 2°. Backgrounds were collected on both sides of the scan. One of three standard reflections was measured every 25 reflections and a maximum random variation of less than 4% was found in all runs.

Intensities were corrected for Lorentz and polarization effects. Individual weights, W, were assigned to the reflections according to $W = l/(\sigma_c^2 + AF_o^2)$ where σ_c is the standard deviation calculated from counting statistics, F_o^2 is the corrected intensity and A is an empirical weighting parameter also determined from counting statistics. Those along with other refinement data are given in Table 5.

Structures were refined using the least-squares program NUCLS6, a modified version of ORFLS (Busing *et al.*, 1962). Atomic scattering factors were interpolated from the tables of Cromer and Mann (1968). Observations less than 3σ were discarded and the structures were refined using F after converting from F^2.

The composition used for refinement was corrected to include the small amounts of Mn and Fe as Mg (see Table 2). Scattering factors for Mg were adjusted accordingly.

The refinement of site occupancies was constrained by bulk composition; full occupancy of all sites was assumed. The 18 independent parameters varied included an overall scale factor, an occupancy parameter for Ca on the A site, the *z* positional parameter for carbon, *x*, *y*, and *z* positional parameters for oxygen, and 12 independent anisotropic thermal parameters (two each for Ca(A), Ca(B) and C, and 6 for O). In addition, an extinction coefficient was varied for EU.

Results

Samples EU, DO-1050, and DO-1100 refined with a dolomite structure (space group $R\bar{3}$). R-factors, positional parameters, anisotropic thermal parameters, cation site occupancies, and thermal ellipsoid data are reported in Tables 5, 6, 7 and 8, respectively. Calculated interatomic distances and angles are given in Table 9. Tables of the observed and calculated structure factors have been

Table 6. Atomic positional parameters and temperature factors for ordered and partially disordered dolomites

Atom	Coord.	EU	DO-1050	DO-1100
		Positional parameters		
C	z	0.24266(5)[1]	0.2436 (2)	0.2442 (2)
O	x	0.24762(9)	0.2483 (4)	0.2516 (3)
	y	-0.03535(9)	-0.0309 (3)	-0.0277 (3)
	z	0.24406(2)	0.24475(9)	0.24514(8)
		Temperature factors		
A Site				
β_{11}[2]		985(9)	1620(44)	1414(39)
β_{33}		60(1)	106(3)	101(3)
B[3]		0.66(1)	1.11(2)	1.00(1)
B Site				
β_{11}		724(17)	1438(73)	1176(60)
β_{33}		56(2)	108(6)	104(5)
B		0.53(1)	1.03(2)	0.90(1)
C				
β_{11}		801(41)	1439(187)	1594(172)
β_{33}		59(2)	102(11)	92(11)
B		0.57(1)	1.01(1)	1.05(1)
O				
β_{11}		839(17)	1682(93)	1731(84)
β_{22}		1400(19)	2182(102)	2555(100)
β_{33}		107(1)	165(6)	178(6)
β_{12}		628(14)	1061(75)	1305(70)
β_{13}		-34(3)	-48(15)	-11(15)
β_{23}		-94(3)	-35(16)	-12(17)
B		0.86(1)	1.43(2)	1.53(1)

[1]Estimated standard errors in parentheses.
[2]$\beta \times 10^5$; anisotropic temperature factors of the form
$$\exp [-(\beta_{11}h^2 + \beta_{22}k^2 + \beta_{33}\ell^2 + 2\beta_{12}kh + 2\beta_{13}h\ell + 2\beta_{23}k\ell)]$$
[3]Equivalent isotropic temperature factor calculated from L. W. Finger's program BONDAN

deposited with the Business Office, MSA[1]. Final difference Fourier maps show average background electron densities of approximately ± 0.2 eÅ^{-3} and no peaks higher than ± 0.4 eÅ^{-3}, indicating that the structures are essentially correct.

Refined parameters for the starting material EU agree closely with those reported by Steinfink and Sans (1959), Althoff (1977) and Effenberger *et al.* (1981) for other stoichiometric dolomites. Occupancy parameters indicate essentially ideal cation order in EU. Positional parameters confirm that the carbon atom deviates slightly from the plane of the oxygen atoms due to the difference in charge density between Ca and Mg (*cf.* Lippmann, 1973).

[1] To obtain a copy of the observed and calculated structure factors, order Document AM-83-231 from the Business Office, Mineralogical Society of America, 2000 Florida Ave., N.W., Washington, D.C. 20009. Please remit $1.00 in advance for the microfiche.

Occupancy parameters for DO-1050 and DO-1100 indicate increasing cation disorder with increasing temperature of equilibration, as anticipated. Similarly, there is an attendant gradual change in lattice parameters and interatomic distances as shown in Figures 1 and 2. The larger uncertainties of refined parameters for the crystals annealed at 1050° and 1100°C reflect the smaller number of independent reflections used (roughly half as many as for EU) and possibly the greater abundance of crystal defects.

Comparison of equivalent isotropic temperature factors (Table 6) reveals large increases for all sites for the partially disordered dolomites relative to the ideally ordered sample. The amount of increase is roughly the same for all sites and no substantial differences between the two partially disordered dolomites are found.

In the dolomite structure, the A and B cation sites and carbon lie on a 3-fold rotation axis. Consequently, the orientation of the thermal ellipsoids is constrained so that one of the principal axes coincides with the rotation axis and the dimensions of the remaining axes are constrained to be equal. In EU the thermal ellipsoids for Ca, Mg, and C are nearly spherical, that for Ca being just slightly oblate and those for Mg and C slightly prolate. Oxygen lies on a general position in dolomite and the thermal ellipsoid is unconstrained. In EU the ellipsoid for oxygen is triaxial and moderately anisotropic. The long axis is approximately perpendicular to the three M–O bonds formed by each oxygen; the short axis is nearly parallel to the C–O bond.

In the partially disordered samples all the ellipsoids are larger than in EU. Dimensions of the principal axes of the ellipsoids for the A and B cation sites and for carbon increase by approximately 30% in both DO-1050 and DO-1100, yet the ellipsoids remain roughly spherical. A slightly larger increase is found in the dimensions of the two shorter axes for the oxygen ellipsoid; the long axis increases by considerably less (~18%). Again, no substantial differences between DO-1050 and DO-1100 are observed. We believe that the larger ellipsoids primarily

Table 7. Site occupancy fractions and order parameters for three dolomites

Sample	A Site		B Site		Order Parameter
	Ca[1]	Mg	Ca	Mg	S[2]
EU	0.9989(4)[3]	0.0011	0.0025	0.9975	0.998(1)
DO-1050	0.9258(14)	0.0742	0.0756	0.9244	0.852(3)
DO-1100	0.8773(12)	0.1227	0.1241	0.8759	0.755(2)

[1]Refined parameter
[2]$S = 2X_{Ca(A)} - 1$
[3]Estimated standard error in parameters

Table 8. Magnitudes and orientations of the principal axes of the thermal ellipsoids of ordered and partially disordered dolomites

Site	Ellipsoid axis r_i	EU rms amplitude[1] A°	Angles (°) with respect to $\underline{a}_1$	$\underline{a}_2$	$\underline{c}$	DO-1050 rms amplitude A°	Angles (°) with respect to $\underline{a}_1$	$\underline{a}_2$	$\underline{c}$	DO-1100 rms amplitude A°	Angles (°) with respect to $\underline{a}_1$	$\underline{a}_2$	$\underline{c}$
A	r_1	0.093(1)[2]	60	60	90	0.119(1)	60	60	90	0.111(1)	60	60	90
	r_3	0.088(1)	90	90	0	0.117(1)	90	90	0	0.115(1)	90	90	0
B	r_1	0.080(1)	60	60	90	0.112(2)	60	60	90	0.102(2)	60	60	90
	r_3	0.085(1)	90	90	0	0.118(2)	90	90	0	0.116(2)	90	90	0
C	r_1	0.084(1)	60	60	90	0.112(5)	60	60	90	0.118(4)	60	60	90
	r_3	0.087(1)	90	90	0	0.115(4)	90	90	0	0.109(4)	90	90	0
O	r_1	0.080(1)	7	113	91	0.116(2)	10	115	81	0.112(2)	2	122	89
	r_2	0.099(1)	85	136	128	0.137(2)	82	151	110	0.149(2)	91	141	114
	r_3	0.128(1)	95	55	142	0.148(2)	83	75	158	0.153(2)	88	70	156

[1] rms amplitude of axis r_2 equals that of r_1 for sites A, B, and C.

[2] estimated standard error in parentheses.

reflect positional disorder associated with the partial cation disorder; although it is probable that larger thermal vibrations will also be a contributing factor. We discuss the role of positional disorder in a subsequent section.

Intensity data were collected for DO-1150 and DO-1200 and efforts were made to refine these data prior to the observation of twin domains in these samples. The structures refined during initial cycles to give large and unsat-

isfactory *R*-factors (13 and 17%, respectively). Further refinement using a dolomite model failed to improve residuals. Following the discovery of transformation-induced twin domains, no further efforts were made to refine the data. The intensity data are, however, found to be consistent with a twin model (also see Reeder and Nakajima, 1982).

Discussion

Cation ordering

The observation of domains in DO-1150 and DO-1200 is important because it establishes the critical temperature

Table 9. Selected interatomic distances (Å) and angles (degrees) for three dolomites

	EU	DO-1050	DO-1100
A Site[1] (Ca>Mg)			
Me - O	2.3802(6)[2]	2.366(2)	2.350(1)
$O_1 - O_2$	3.2972(11)	3.280(3)	3.253(3)
$O_1 - O_6$	3.4338(10)	3.411(3)	3.393(3)
$O_1 - Me - O_2$	87.67(2)	87.75(7)	87.58(6)
$O_1 - Me - O_6$	92.33(2)	92.25(7)	92.42(5)
B Site (Mg>Ca)			
Me - O	2.0839(5)	2.106(2)	2.114(2)
$O_1 - O_2$	2.9023(9)	2.936(4)	2.943(3)
$O_1 - O_6$	2.9910(9)	3.021(3)	3.035(3)
$O_1 - Me - O_2$	88.28(2)	88.35(8)	88.24(6)
$O_1 - Me - O_6$	91.72(2)	91.65(8)	91.76(7)
CO_3 Group			
C - O	1.2826(6)	1.274(2)	1.281(2)
O - O	2.2220(9)	2.206(4)	2.218(3)
O - C - O	119.97(1)	119.98(4)	119.99(4)

[1] Oxygens labelled according to convention adopted by Oh et al. (1973) and Althoff (1977).

[2] Estimated errors in parentheses.

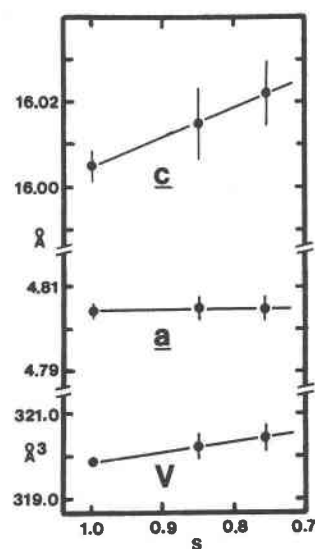
Fig. 1. Unit cell parameters and cell volume plotted as a function of the refined order parameter S. Vertical bars represent errors.
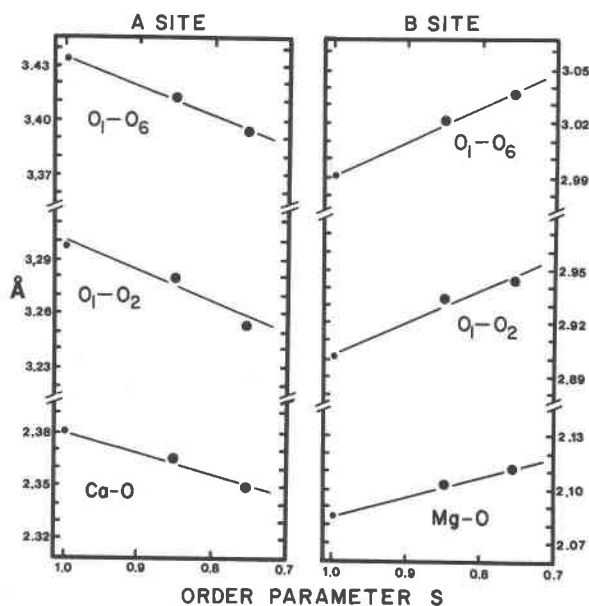
Fig. 2. Selected interatomic distances for the A and B octahedral sites plotted as a function of the order parameter S. The size of the circle reflects the error of the measurement.

($T_{critical}$) of the symmetry change from $R\bar{3}c$ to $R\bar{3}$. In principle, this corresponds to the critical temperature for long-range order, as well. Clearly DO-1050 and DO-1100, lacking domains, did not reach $T_{critical}$ while DO-1150 and DO-1200 surpassed it. As noted previously, DO-1150 and DO-1200 may deviate slightly from ideal stoichiometry, since trace amounts of CaO were found in the powder fractions of these run products. If their compositions have changed, this may slightly alter $T_{critical}$ for these materials relative to stoichiometric dolomite (cf. Goldsmith and Heard, 1961). In order to clarify this, an additional experiment was subsequently run at 1150°C and 15kbar; no CaO or any other evidence of decomposition was observed in the run products. Domains identical to those in DO-1150 and DO-1200 were found, thereby confirming an upper limit of 1150°C for $T_{critical}$.

Intensity data for DO-1150 and DO-1200 indicate significant degrees of cation order since relative intensities of superstructure reflections are only slightly less than those for DO-1100. Thus reordering clearly occurred during the quench. It is difficult to evaluate the extent of reordering since the cation site occupancies were not refined for these specimens. We are forced to acknowledge that DO-1050 and DO-1100 must also have reordered during the quench. Therefore, the refined cation distributions for these specimens represent *minimum* degrees of disorder at their respective equilibration temperatures. Furthermore, the extent of reordering may be significant if one considers that the long-range order parameter[2] S = 0 at

---

[2] $S = 2X_{Ca(A)} - 1$

some temperature less than 1150°C and yet the refined order parameter for DO-1100 is 0.75. This evidence seems to indicate a relative ease of mobility for Ca and Mg in this structure at high temperatures.

Structural changes

If we restrict our observations to EU, DO-1050, and DO-1100, several conclusions can be made about structural changes accompanying disorder, even though the range of disorder represented is rather limited. In Figures 1 and 2 the changes in lattice parameters and selected interatomic distances are shown to be gradual and roughly linear with degree of disorder. If one assumes a linear relationship, it is possible to estimate lattice parameters and cell volume for complete disorder by extrapolation. Values obtained are $a = 4.805$Å, $c = 16.071$Å, and $V = 321.34$Å^3. These should be taken with some caution since considerable extrapolation is required and errors are somewhat large. For complete disordering we estimate $\Delta c = 0.07$Å which is roughly twice the value suggested by Goldsmith et al. (1961) ($\Delta c = 0.03$Å). The latter value is a minimum value, however, since the specimens used by Goldsmith et al. were only partially disordered. Within the error of our measurements we estimate no meaningful change in the a cell parameter. The estimated volume change is $\Delta V = 1.46$Å^3 or 0.46% of the cell volume, compared to $\Delta V = 0.3$Å^3 from Goldsmith et al. The volume change is quite small and pressure should have little effect on either the order-disorder process or $T_{critical}$.

Gradual and progressive changes are *not* observed in interatomic angles between cations and coordinating oxygens as disorder increases. In fact, DO-1050 and DO-1100 show opposing changes relative to EU, although small (Table 9). We can offer no explanation for this behavior at this time since other changes are rather uniform. The angles, however, seem to indicate a different sense of distortion of the octahedra in the respective crystals, possibly an artifact of the rapid quenching and reordering. We also note that the C–O bond length for DO-1050 is somewhat shorter than expected (cf. Zemann, 1981).

Also significant are the changes in the influence of cation ordering on the CO_3 groups. In calcite, with only one cation type and one cation site to occupy, the net change density effects on a CO_3 group are uniform owing to the presence of identical cation layers above and below the CO_3 layer. Thus oxygen atoms assume positions equidistant between the two nearest-neighbor Ca atoms, one each from the upper and lower cation layers. The C–O bond direction is then parallel to the a-axis. In ideal dolomite, charge densities for Ca layers differ significantly from adjacent Mg layers. Oxygen atoms then assume positions closer to Mg than Ca and the net result is that CO_3 groups are uniformly rotated around the 3-fold axis by roughly 6.6° away from the position assumed in calcite. The C–O bond is misaligned by 6.6° from the a-axis and this, of course, violates the c-glide found in the calcite structure (the cation ordering does as well). As disorder

begins to occur the local cation configuration around a CO_3 group will change, many different configurations being possible. The net effect of increasing disorder will be to decrease the *average* angle of rotation toward zero. The calculated angle of rotation for EU, 6.6°, decreases to 5.8° and 5.2° for DO-1050 and DO-1100, respectively.

Similarly, in ideal dolomite the unequal charge densities of the Ca and Mg layers force the carbon atom out of the plane of the oxygen atoms (the CO_3 group is planar in calcite). In EU the displacement along c is 0.022Å and decreases to 0.018Å and 0.014Å in DO-1050 and DO-1100, respectively.

Local variations in cation configurations associated with partial cation disorder appear to be the most probable cause for the observed large thermal parameters of DO-1050 and DO-1100. This local variability results in greater variability in bond lengths (and angles) and hence positional disorder. Thus we interpret the large thermal ellipsoids in DO-1050 and DO-1100 as representing positional disorder to some degree.

Twinned crystals

We note one final observation from the intensity data of DO-1150 and DO-1200. Both Fourier and difference Fourier maps revealed 3 extra peaks corresponding exactly to the position and configuration of a normal CO_3 group, but rotated by 180° around the 3-fold axis (Fig. 4 in Reeder, 1980). These peaks have electron densities of less than one-tenth the density for a normal oxygen position; densities observed in DO-1200 are slightly greater than those in DO-1150. We believe that these peaks may represent CO_3 group disorder of a rotational type. The disorder is *not* directly related to the twin domains since peak densities are both too small and in the wrong positions for the observed domains. The disorder may possibly be an artifact of the rapid reorganization of the atoms during the quench (none were observed in DO-1050 or DO-1100, however). Alternatively we can speculate that the disorder might also be an artifact of an equilibrium, thermally-induced, rotational disorder. Presumably such disorder would not be quenchable. However, it is possible that a few localized domains might form with CO_3 groups out of phase. Such disorder remains speculative, although not unreasonable, considering that thermally-induced NO_3 group disorder is well documented in $NaNO_3$ (Paul and Pryor, 1971), and similar CO_3 group disorder is strongly suggested in experiments on calcite by Mirwald (1979a, b).

Summary

Structure refinements of the annealed dolomites provide new data on structural changes accompanying cation disordering. The increased disorder at higher temperatures induces gradual shifts in most structure-sensitive parameters. Such changes are consistent with a continuous transformation mechanism. However, a first-order transformation cannot be entirely ruled out, since reordering during quenching prevented recovering completely disordered samples. Cation disorder is predicted to be complete by 1150°C. We know of no alternative technique which can overcome this quenching problem. This leaves *in situ* measurements as the only alternative, for example, with a diamond-anvil cell. Future advances in that field may make such measurements possible.

References

Althoff, P. L. (1977) Structural refinements of dolomite and a magnesian calcite and implications for dolomite formation in the marine environment. American Mineralogist, 62, 772–783.

Barber, D. J., Heard, H. C. and Wenk, H. R. (1981) Deformation of dolomite single crystals from 20–800°C. Physics and Chemistry of Minerals, 7, 271–286.

Busing, W. R., Martin, K. O., and Levy, H. A. (1962) ORFLS, a Fortran crystallographic least-squares refinement program. U. S. National Technical Information Service, ORNL-TM-305.

Cromer, D. T. and Mann, J. B. (1968) X-ray scattering factors computed from numerical Hartree–Fock wave functions. Acta Crystallographica A, 24, 321–324.

Effenberger, H., Mereiter, K., and Zemann, J. (1981) Crystal structure refinements of magnesite, calcite, rhodochrosite, siderite, smithonite, and dolomite, with discussion of some aspects of the stereochemistry of calcite type carbonates. Zeitschrift für Kristallographie, 156, 233–243.

Goldsmith, J. R. (1959) Some aspects of the geochemistry of carbonates. In P. H. Abelson, Ed., Researches in Geochemistry, p. 336–358. Wiley, New York.

Goldsmith, J. R. (1972) Cadmium dolomite and the system $CdCO_3$–$MgCO_3$. Journal of Geology, 80, 617–626.

Goldsmith, J. R. (1980) Thermal stability of dolomite at high temperatures and pressures. Journal of Geophysical Research, 85, 6949–6954.

Goldsmith, J. R. and Graf, D. L. (1958) Structural and compositional variations in some natural dolomites. Journal of Geology, 66, 678–693.

Goldsmith, J. R. and Heard, H. C. (1961) Subsolidus phase relations in the system $CaCO_3$–$MgCO_3$. Journal of Geology, 69, 45–74.

Goldsmith, J. R., Graf, D. L., and Heard, H. C. (1961) Lattice constants of the calcium-magnesium carbonates. American Mineralogist, 46, 453–457.

Irving, A. J. and Wyllie, P. J. (1975) Subsolidus and melting relationships for calcite, magnesite and the join $CaCO_3$–$MgCO_3$ to 36kb. Geochimica et Cosmochimica Acta, 39, 35–53.

Lippmann, F. (1973) Sedimentary Carbonate Minerals. Springer-Verlag, New York.

Mirwald, P. W. (1979a) Determination of a high-temperature transition of calcite at 800°C and one bar CO_2 pressure. Neues Jahrbuch für Mineralogie, Monatschefte, 7, 309–315.

Mirwald, P. W. (1979b) The electrical conductivity of calcite between 300 and 1200°C at a CO_2 pressure of 40 bars. Physics and Chemistry of Minerals, 4, 291–297.

Navrotsky, A. and Loucks, D. (1977) Calculation of subsolidus phase relations in carbonates and pyroxenes. Physics and Chemistry of Minerals, 1, 109–127.

Oh, K. D., Morikawa, H., Iwai, S., and Aoki, H. (1973) The crystal structure of magnesite. American Mineralogist, 58, 1029–1033.

Paul, G. L. and Pryor, A. W. (1971) The study of sodium nitrate by neutron diffraction. Acta Crystallographica B, 27, 2700–2702.

Reeder, R. J. (1980) Phase Transitions in Dolomite. Ph.D. Thesis, University of California, Berkeley.

Reeder, R. J. and Nakajima, Y. (1982) The nature of ordering and ordering defects in dolomite. Physics and Chemistry of Minerals, 8, 29–35.

Steinfink, H. and Sans, F. T. (1959) Refinement of the crystal structure of dolomite. American Mineralogist, 44, 679–682.

Zachariasen, W. H. (1967) A general theory of x-ray diffraction in crystals. Acta Crystallographica, A23, 588–564.

Zemann, J. (1981) Zur Stereochemie der Karbonate. Fortschritte der Mineralogie, 59, 95–116.